Helium atom scattering experiments and molecular dynamics simulations of the structure and lattice dynamics of 15-layer acetylene films on KCl(001)

J. P. Toennies and F. Traeger*
Max-Planck-Institut für Strömungsforschung, Bunsenstraße 10, D-37073 Göttingen, Germany

H. Weiss
Chemisches Institut der Otto-von-Guericke-Universität, Universitätsplatz 2, D-39106 Magdeburg, Germany

S. Picaud and P. N. M. Hoang
Laboratoire de Physique Moléculaire–UMR CNRS 6624, Faculté des Sciences, La Bouloie, Université de Franche-Comté, F-25030 Besançon Cedex, France

(Received 13 November 2001; published 10 April 2002)

The surface structure and lattice dynamics of thick films of 15 to 40 layers of acetylene adsorbed on a KCl(001) single crystal surface have been investigated at about 40 K by combining helium atom scattering (HAS) experiments with classical molecular dynamics simulations. As rarely occurs for physisorbates on ionic crystals layer-by-layer growth is observed by HAS up to at least 15 layers producing films with a $(\sqrt{2}\times\sqrt{2})R45°$ geometry. The simulations confirm the stability and structure of these layers up to about 100 K. The time-of-flight spectra reveal along the [110] direction at least four phonon modes, which are assigned by simulations based on the calculated power spectra of the velocity and angular autocorrelation functions.

DOI: 10.1103/PhysRevB.65.165427 PACS number(s): 68.35.Ja, 68.35.Bs

I. INTRODUCTION

The acetylene molecule C_2H_2 (also called ethyne) is the smallest of all stable hydrocarbons and thus is an ideal model system.[1] Thick multilayered films of the hydrocarbons are of interest in connection with (i) photolytic reactions as for example recently observed in a 150 K lattice gas phase of acetylene on NaCl(001),[2,3] (ii) understanding the elementary processes involved in lubrication,[4] and (iii) the quantum Hall effect, superconductivity and electrically pumped laser emission, recently observed in the surface layers of tetracene and pentacene crystals.[5,6] In the past most of the structural and phonon studies of thin films on insulators in vacuum have been restricted to disordered films or to monolayers. The only experimental structural studies of thicker crystalline films on insulators that we are aware of are the neutron diffraction experiments of Bienfait, Suzanne, and Coulomb and collaborators.[7–9] In these experiments the films are grown on the (001) face of microcrystallites of MgO powders at pressures of tens of millitorrs.

In the present article the results on the successful growth of thick single crystal films of acetylene consisting of 15-40 layers are described. The structure and surface vibrational modes were studied using helium atom scattering (HAS). As demonstrated in several previous publications[10–12] helium atom scattering appears to be the optimal technique for investigating physisorbed films especially on nonconducting insulator surfaces. Being neutral there are no space charge problems with He atoms. Moreover, because of the low collision energies ($\leqslant 60$ meV) HAS is both nondestructive and uniquely sensitive to the top-most surface. The high inherent monochromaticity and intensity of the helium atom beams facilitate both structural determinations via diffraction and the measurement of surface phonon dispersion curves via time-of-flight (TOF) spectroscopy.[13]

In three previous publications the structures and lattice dynamics of monolayers of acetylene on NaCl (Refs. 10,11) and on KCl (Ref. 12) were studied with HAS. The lattice mismatch of 8% in the case of NaCl explains the presence of two phases, which provide two different ways to relieve the induced stress. At a surface temperature of $T_S=50$ K a buckled monolayer possessing a $(\sqrt{2}\times 7\sqrt{2})R45°$ symmetry with a glide plane with a periodicity of 39.5 Å is found.[10] At $T_S=80$ K the molecule density is reduced to 2/3 of a monolayer by the formation of isolated stripes consisting of alternating 90° rotated molecules. The structures of both phases and the lattice dynamics of the lower density high temperature phase are in good agreement with a subsequent theoretical analysis based on potential energy optimization and lattice dynamics calculations.[11] For KCl the smaller mismatch of only 1.8% with respect to bulk acetylene explains the simple $(\sqrt{2}\times\sqrt{2})R45°$ registry observed in the diffraction patterns.[12] In addition the TOF spectra provide evidence for at least four different strongly dispersive modes below 14 meV. Molecular dynamics simulations based on semiempirical potentials were used to determine the equilibrium structure. The lattice dynamics simulations, similar to those in Ref. 11, lead to the assignment to frustrated stretch vibrations (S mode) and frustrated rotations (librons) and frustrated translational modes (T modes) with a strong hybridization with the substrate vibrations.

In Sec. II the experimental apparatus and the results of the helium scattering experiments will be presented. In Sec. III this is followed by a description of the theoretical method. The theoretical results are presented in Sec. IV and are compared with the experiment in Sec. V. The final Sec. VI closes with a brief summary of the results.

II. EXPERIMENT

A. Experimental setup

The apparatus is essentially identical to that used in the previous experiments[10–12]. A nearly monoenergetic He atom beam [full width at half maximum (FWHM): $\Delta v/v \sim 1\%; \Delta E/E \sim 2\%$] is generated by continuous free jet expansion of He gas through a nozzle of 10 μm in diameter from a stagnation pressure of 50–400 bar into vacuum. In the present work beam energies between 10 and 29 meV, corresponding to nozzle temperatures between 50 and 135 K, were used. After scattering from the sample the He atoms are detected by a mass spectrometer at the end of a 1.428 m long flight tube. The angle between incident and final scattered beams is fixed to $\theta_i + \theta_f = 90.1°$, where θ_i and θ_f are the incident and final angles measured with respect to the surface normal. Angular distributions are measured by rotating the crystal around an axis perpendicular to the scattering plane (polar rotation) thereby varying both the incident and final angles. The angular distributions are converted to parallel wave vector changes given by $\Delta K = k_f \sin\theta_f - k_i \sin\theta_i$, where k_i and k_f are the incident and final wave vectors. Different crystal azimuthal directions are aligned by rotating the crystal surface around an axis parallel to the scattering plane. For time-of-flight measurements the helium atom beam is chopped with a variable-speed, variable-pulse-width chopper. The time-of-flight spectra are converted to an energy scale (ΔE) by combining the conservation of energy and momentum according to the ''scan curve''[13,14]

$$\frac{\Delta E}{E_i} = \frac{\sin^2(\theta_i)}{\sin^2(\theta_f)}\left(\frac{\Delta K}{K_i} + 1\right)^2 - 1, \qquad (1)$$

additional experimental details may be found in Ref. 14.

The KCl surfaces were prepared by cleaving off a small slice from a KCl single crystal with 10×10 mm^2 surface area at a surface temperature of 100 K *in situ* under UHV conditions in the 10^{-11} mbar range. After cleavage and between measurements the crystal was maintained at 400 K to prevent possible deterioration of the surface quality by residual water vapor. The acetylene gas (Messer-Griesheim GmbH, purity 99.6%, main impurity acetone) was purified in 5–6 cycles of condensation of the acetylene in a liquid-N_2 trap, pumping the gas line to remove volatile impurities like hydrogen, and warming up the cold trap. During gas dosage any remaining acetone was frozen out in a cold trap filled with a mixture of *n*-pentane and liquid N_2 at 143 K. The sample temperature was measured by means of a NiCr/Ni thermocouple which was embedded into the crystal by inserting it into a hole drilled into one side and plugging the hole up with KCl powder. The sample was cooled by liquid helium and the target temperatures were stabilized better than to ± 0.1 K by a computer-regulated heater in the sample holder, whereas the absolute accuracy of the temperature measurement is estimated to be around ± 1 K.

B. Experimental Results

In order to prepare well-ordered adsorbate layers, the KCl(100) single crystal was exposed to 2.5×10^{-8} mbar acetylene gas at a sample temperature of 40 K. In Fig. 1 the intensity of the specularly reflected He beam is shown as a function of the exposure time *t*. The initial steep decrease in intensity is mostly due to incoherent scattering from the first adsorbed molecules which act as single isolated defects on the KCl surface with large scattering cross sections.[15] Then after about 370 s the intensity recovers slightly as the spaces between the single adsorbate molecules are filled and coherent patches appear. The first weak maximum indicated by an arrow is attributed to the completion of the first monolayer.[12] The first weak maximum is followed by at least eleven regularly spaced maxima with varying amplitudes. This behavior indicates a layer-by-layer growth of the adsorbate in which each maximum corresponds to the completion of an acetylene layer corresponding to a minimum in defect density.[15] Towards the end of the adsorption curve the oscillation amplitudes become smaller and smaller due to a growing amount of defects in the full layers and therefore a smaller difference in defect density between full and partially filled layers.

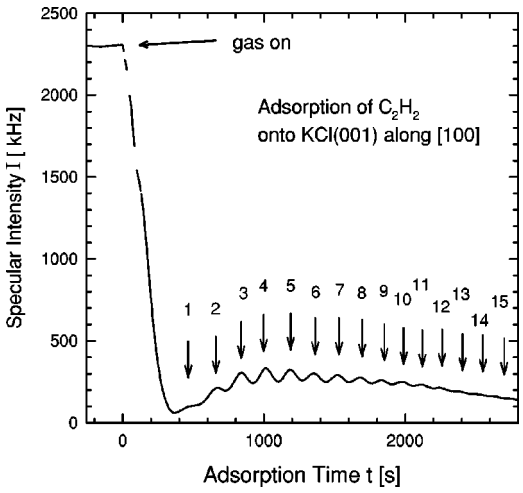

FIG. 1. Specular intensity during isothermal adsorption of acetylene on KCl(001) measured along the [100] crystal direction at a surface temperature of $T_S = 40$ K and an acetylene pressure 2.5×10^{-8} mbar with an incident wave vector of $K_i = 5.4$ Å^{-1}. The regular oscillations in the multilayer regime indicate layer-by-layer growth of the adsorbate.

After adsorption at $T_S = 40$ K, and prior to the diffraction and time-of-flight experiments, the multilayer adsorbate was usually annealed for 20–30 min at $T_S = 60$ K. The annealing resulted in an increase of the diffraction intensity by a factor of at least 2, sometimes up to 5, which is probably due to a smoothing of the topmost layers. Changes in surface coverage as well as adlayer symmetry due to the annealing could be excluded by comparing angular distribution and time-of-flight measurements of layers prepared with and without annealing as well as routinely observing the specular intensity during the annealing process. In this way well structured surfaces with up to 40 layers could be prepared.

In Fig. 2 the time for the appearance of the first eleven successive maxima is plotted as a function of the number n of the maximum. For the third and higher maxima, i.e., in the multilayer regime, it takes about 160 s, corresponding to a

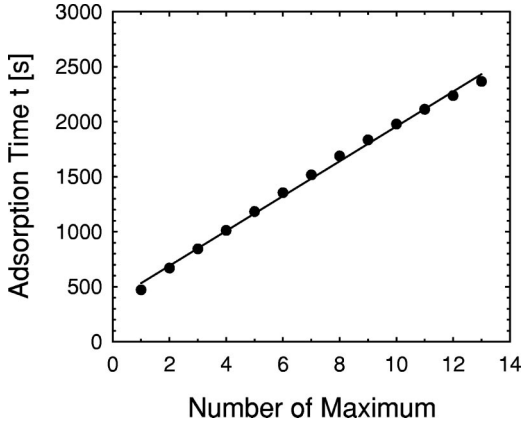

FIG. 2. Exposure time as a function of the number of each maximum in specular intensity. A maximum corresponds to the completion of an acetylene layer.

dosage of 3 L to form the next layer. Under the reasonable assumption of one acetylene molecule per KCl surface lattice unit cell this corresponds to a sticking coefficient of about 0.4. In contrast, the first three maxima seen prior to the multilayer regime are not regularly spaced and appear after longer adsorption times. One possible interpretation for this irregularity implies that the time for layer completion is the same for all layers, i.e., the sticking coefficients are constant. In this case, during the adsorption of the first four layers, only two maxima would be observed, indicating either the filling of a layer before the underlying one is complete, or the formation of bilayers. In the second possible explanation each maximum corresponds to the completion of one layer and there is a variation of the sticking coefficients. If the third $n=3$ maximum at $t=844$ s corresponds to the completion of the third layer, then the sticking coefficient for the first layer is only 0.15, for the second layer 0.3 and for higher layers 0.4. An argument in favor of this second possibility is the softness of the multilayers, which increases with their thickness. The softer the layer, the more low-frequency phonons are available to thermalize an acetylene molecule colliding with the surface, and hence enhancing the sticking probability. Indeed, the surface Debye temperature of 15 layers C_2H_2 extracted from the attenuation of the elastically scattered He signal with increasing incident energy is (88 ± 20) K, which is more than 20% below the Debye temperature (Θ_D) of the monolayer and 45% less than that of the substrate ($\Theta_D=160$ K), which has also been measured in this study.

From desorption temperatures of 81–82 K, measured by monitoring the increase in specular intensity while heating the crystal, a binding energy of (250 ± 10) meV per molecule in the multilayer regime can be estimated using the Redhead formula.[16]

The symmetry of the adsorbate layers (with respect to the substrate) was determined from the He atom angular distributions along the [110], [100], [310], and [210] azimuthal crystal directions shown in Fig. 3. All the diffraction patterns—with the exception of the [210] direction—are dominated by peaks with the same periodicity as the substrate. Along the [210] azimuth the half-order superstructure

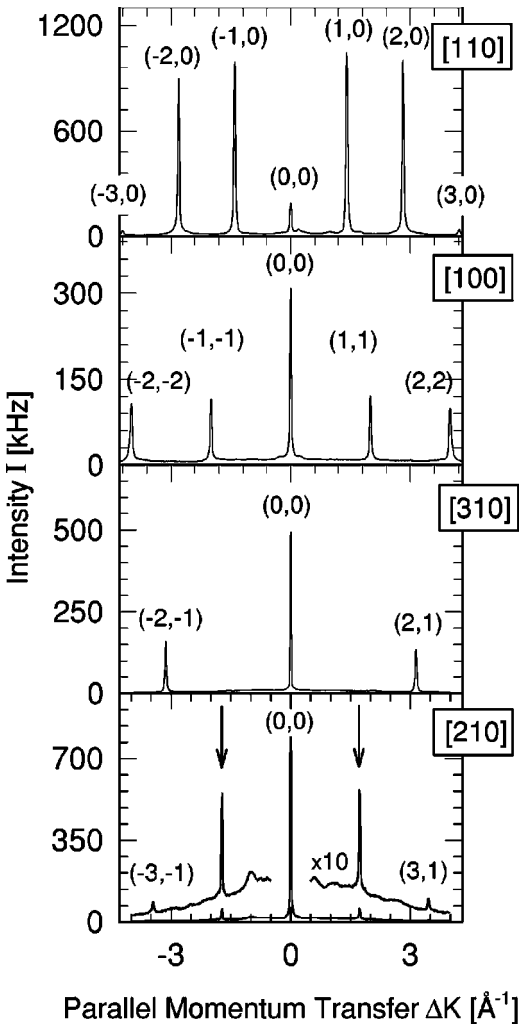

FIG. 3. Angular distributions of 15 layers acetylene on KCl converted to a parallel momentum scale measured along the [110], [100], [310], and [210] azimuthal directions. The measurements along [110] and [100] were taken with an incident wave vector of $k_i=5.3$ Å^{-1} and those along [310] and [210] with $k_i=4.9$ Å^{-1}. Only along [210] are half-ordered superstructure peaks visible, which are marked with arrows. From these diffraction scans a $(\sqrt{2}\times\sqrt{2})R45°$ symmetry of the surface unit cell can be deduced.

peaks indicate a $(\sqrt{2}\times\sqrt{2})R45°$ superstructure with glide planes along the [100] and [010] directions in the multilayer adsorbate lattice unit cell, as found previously for the monolayer.[12] The corresponding reciprocal lattice as well as the real space unit cell are shown in Fig. 4. The twofold glide plane symmetry, which is indicated by the absence of half-order diffraction peaks along the [100] azimuthal direction, requires a flat orientation of the molecules with respect to the surface. This structure is consistent with a face of the orthorhombic modification of bulk acetylene, which is the stable modification in the temperature range of the experiment.[17] It has also been found by means of infrared spectroscopy of acetylene layers on KCl prepared under the same conditions.[18] In this plane, the lattice vectors of the two high symmetry directions of the orthorhombic structure, which are rotated by 90° with respect to each other, differ by $\sim 3\%$

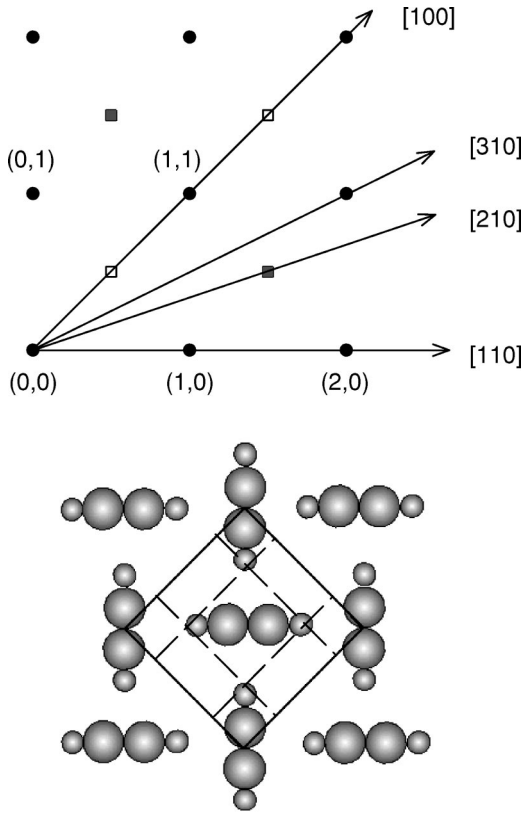

FIG. 4. Reciprocal lattice and real space unit cell of the acetylene multilayer surface. The solid line shows the surface unit cell. The dashed lines correpond to glide planes which are indicated by missing half-order diffraction peaks along the [100] azimuthal directions.

from each other, and are about 0.8 and 3.6% smaller than the KCl lattice vector. Because of this relatively good fit it is likely that the adsorbate forms an orthorhombic surface cell, which is very close to the cubic symmetry of the KCl substrate. Unfortunately a unique experimental confirmation of this structure is not possible. Although the apparative resolution is adequate to resolve at least a 3.6% misfit, the multilayer diffraction peaks are too broad to distinguish between a cubic and an orthorhombic phase. The specular peak width $\delta\Delta K$ between 0.024 and 0.055 Å^{-1}, which is significantly larger than observed for the bare substrate as well as for the monolayer, is probably due to rather small domains of only $\Delta x = 10-25$ nm in diameter, as estimated using the relation $\Delta x = 2\pi/\delta\Delta K$.

The dynamical properties of the acetylene layers were determined from the time-of-flight spectra of inelastically scattered He atoms from the surface. Most of the 108 time-of-flight spectra were taken on adsorbates of 15 layers thickness, which had been prepared under the conditions given above. In addition, measurements at 40 layers thickness rule out a coverage dependence of the energy transfers. Essentially the same structure of the TOF spectra is found for this coverage as well, with only slightly different relative intensities of the peaks. The frequencies of organ pipe modes, which have been found for example in alkali metal layers on different metal substrates (see, e.g., Ref. 19) are

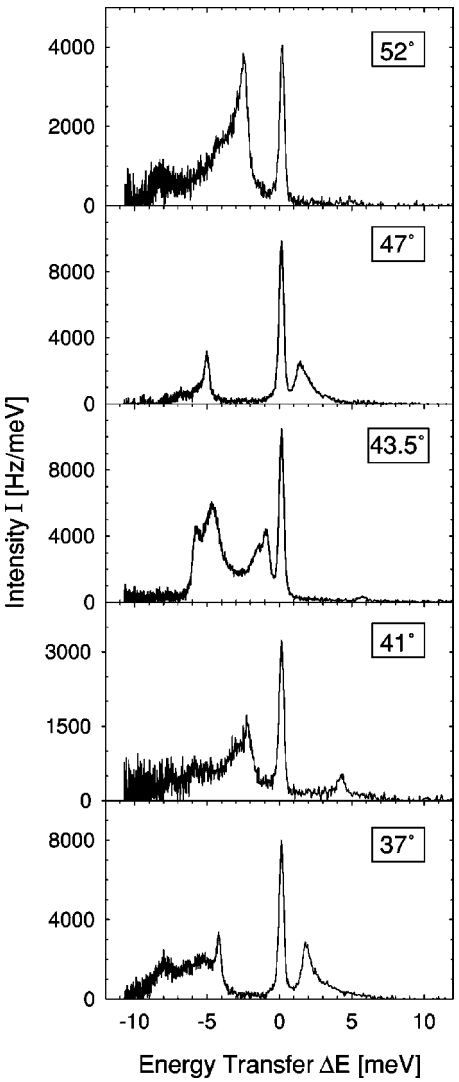

FIG. 5. Examples of time-of-flight spectra of 15 layers acetylene on KCl. The incident energy was $E_i = 14.9$ meV and the surface temperature $T_S = 40$ K. The time-of-flight scale has been converted to an energy scale.

dependent on the thickness of the layer. Therefore the comparison between measurements of 15 layers and 40 layers also rules out the presence of organ pipe modes.

Figure 5 shows some typical time-of-flight spectra of 15 layers C_2H_2/KCl converted to an energy scale, which have been measured along [110] at incident angles between $\theta_i = 37°$ and 52°. The surface temperature was $T_S = 40$ K and the incident He beam energy was 14.9 meV. In each spectrum the inelastic He signal was integrated over 1×10^6 (at 41°, 43.5°, and 47°) or 1.5×10^6 (37° and 52°) time-of-flight cycles corresponding the measuring times of 33 and 50 min, respectively. The intensities, however, cannot be compared directly, since the figure contains spectra from different series. For each of the series, a fresh layer was prepared and the absolute intensities varied between these adsorbates, which is probably due to not perfectly reproducible defect densities of these layers.

Figure 6 shows the measured phonon dispersion curves for a 15 layer acetylene film along the [110] direction of the

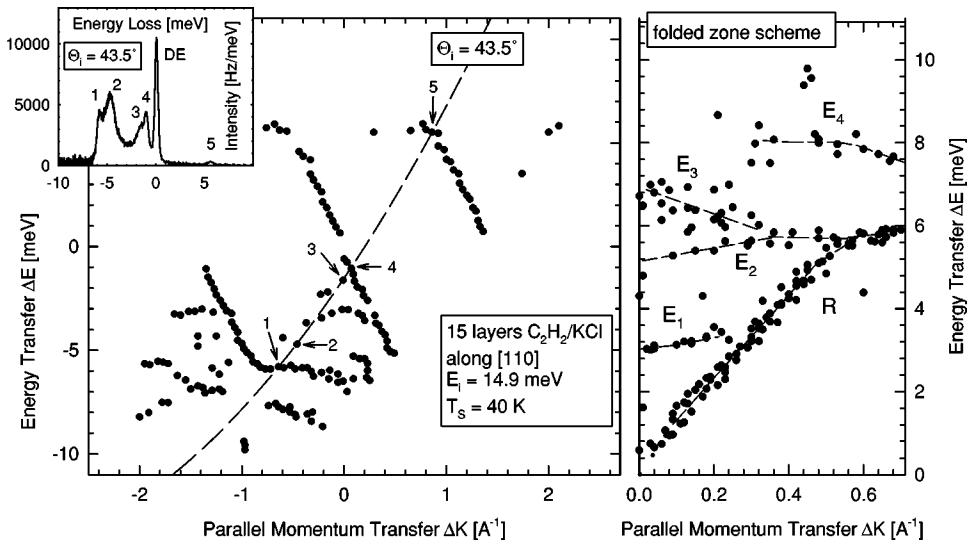

FIG. 6. Dispersion curve of the surface phonons of 15 layers of acetylene measured along the [110] direction at an incident energy of $E_i = 14.9$ meV and a surface temperature of $T_S = 40$ K. The left panel shows the data in an unfolded zone scheme, the right panel in a folded zone scheme. The inset on the left shows a time-of-flight spectrum for the incident angle of $\Theta_i = 43.5°$, which is displayed on an energy scale. The energy transfers of this spectrum are assigned with the aid of the appropriate scan curve shown as a dashed line in the figure. The dashed line in the folded zone scheme serve as guide to the eye only.

KCl substrate crystal compiled from 41 time-of-flight spectra between incident angles of 35° and 55°. In Fig. 6 (left) the data are shown in an unfolded zone scheme together with a sample time-of-flight spectrum and its corresponding scan curve for $\theta_i = 43.5°$. In Fig. 6 (right), the dispersion curves have been folded back into the first Brillouin zone. The most pronounced mode is a dispersive mode between nearly 0 meV at the zone center and 6 meV at the zone boundary. Based on a comparison with the calculations of the bulk acetylene crystal phonons by Gamba and Bonadeo,[20] it is assigned to the Rayleigh mode *R* of the acetylene surface. Their calculated values for the slope of the transverse acoustic mode in the first part of the Brillouin zone, 8.8 meV/Å^{-1}, and its energy at the zone boundary, 6.2 meV, agree reasonably well with the values of 9.8 meV/Å^{-1} and 5.8 meV measured here. The agreement between the zone boundary energies may be even better, since from the experimental data it is not clear, whether the Rayleigh mode is cut by another nearly dispersionless mode above $\Delta K \approx 0.55$ Å^{-1} and hence not observed at higher parallel momentum transfers.

In addition to the Rayleigh phonon, at least three additional modes are found. Starting from lowest energies, a phonon (E_1) is identified around 3.0 meV in the first third of the Brillouin zone, i.e., in the bulk band region. The fact that it is only seen close to the zone origin suggests a significant contribution of motions perpendicular to the surface.[12] At higher energies between 5 and 7 meV two or possibly even more weakly dispersive modes are detected (E_2 und E_3), which seem to coalesce at parallel momentum transfers $\Delta K > 0.3$ Å^{-1}. Very likely they hybridize with the Rayleigh mode, as frequently observed in other systems (see, e.g., Ref. 21). If this is the case, the modes E_2 and E_3 would be continued in the region where the coupling with the substrate is not allowed, while the continuation of the Rayleigh mode is not observable for these values of ΔK. A fourth phonon (E_4) is detected around 8 meV close to the zone boundary, the latter being an indication for a dominantly parallel polarization. However, due to the scatter in the data it is also possible that this mode extends throughout the whole Brillouin zone.

Time-of-flight spectra along the [100] direction show similar structures. However, as has been found for the monolayer as well, the time-of-flight spectra along this direction are of poorer quality, which is mostly due to additional peaks from selective adsorption resonances.

III. MOLECULAR DYNAMICS SIMULATIONS

A. Interaction potential

The total interaction potential between the acetylene molecule and the KCl substrate is written as a sum of molecule-substrate V^{MS} and lateral molecule-molecule V^{MM} potential terms. Each of these potentials consists of electrostatic and dispersion-repulsion contributions. The definition of V^{MS} is based on our previous work on the monolayer of acetylene adsorbed on KCl.[12] The electrostatic contribution originates from the interaction between the charges $\pm e$ (e is the electron charge) of the substrate ions and the single point quadrupole moment (equal to 7.2 DÅ) (Ref. 22) of the acetylene molecule. The dispersion-repulsion interactions in V^{MS} are described by site-site pairwise Lennard-Jones potentials between the C, H, K, and Cl nuclei. The values of the corresponding parameters ϵ and σ are taken from Ref. 12. The induction terms which account for the mutual polarization of the substrate and of the admolecules are less than 10–15 % of the other contributions.[12]

For the lateral interaction V^{MM} between acetylene molecules, we use the model of Leech and Grout.[23] In this

TABLE I. Potential parameters for the lateral interactions between acetylene molecules. The electrostatic parameters are given in atomic units whereas the dispersion-repulsion parameters are given in meV and Å.

site	charge	dipole	quadrupole
center of mass	−0.1546		0.4061
C	0.0137	±0.3328	−0.1926
H	0.0636	±0.0724	0.2826
atomic pair	C_6 (meV· Å^6)	A (meV)	α(Å^{-1})
C-C	20536.1	3823924.5	3.671
H-H	477.3	367345.8	4.222
C-H	2260.1	731578.5	4.019

model, the charge distribution of the acetylene molecule is described by a set of multipoles, up to the quadrupole moment, localized on the C and H atoms, and on the center of mass of the molecule. These distributed multipoles account for the nonlocal electronic extension of the molecule, and accurately reproduce the total point quadrupole moment of C_2H_2. In addition, the model also contains three exp-6 functions representing the C-C, H-H, and C-H repulsion-dispersion interactions. Note that such a combination of distributed multipole moments and exp-6 forms is required to give the structure and the dynamics of both orthorhombic and cubic phases of bulk acetylene.[23,24] The parameters of this model are summarized in Table I.

The total interaction potential between the C_2H_2 admolecules and the KCl substrate is then written as

$$V=\sum_i \left[\sum_{l,s,p} V^{\mathrm{MS}}(\mathbf{r}_{ilsp},\mathbf{\Omega}_i)+\sum_{j\neq i} V^{\mathrm{MM}}(\mathbf{r}_{ij},\mathbf{\Omega}_i,\mathbf{\Omega}_j)\right], \tag{2}$$

where $\mathbf{r}_{ilsp}$ is the distance vector between the center of mass of the molecule i and an atom s of the lth unit cell in a plane p of the substrate, and $\mathbf{r}_{ij}$ is the distance vector between two atoms belonging to the ith and jth molecules. $\mathbf{\Omega}_i$ describes the orientation of the ith acetylene molecule in an absolute coordinate system.

B. Details of the simulation

In the molecular dynamics simulations used to determine the structure of the acetylene adsorbate at finite temperature the ionic substrate is represented by six rigid layers of K^+ and Cl^- ions arranged according to the (001) geometry, which occupy the bottom of the simulation box. To be consistent with the experiments, the simulation box contains between 1 and 15 layers of moving acetylene molecules adsorbed on KCl, thus forming a film of up to 43.0 Å thickness along the **z** axis normal to the surface ($z=0$ located at the KCl surface). The (x,y) size of the simulation box ($x=y=35.04$ Å, parallel to the KCl surface) corresponds to a repeated patch of size $8a_s\times 8a_s$ (where $a_s=4.38$ Å is the substrate unit cell parameter). At the beginning of the simulation, the innermost acetylene layer has a flat geometry with one C_2H_2 molecule per substrate cation site, and thus contains 64 acetylene molecules arranged in a $(\sqrt{2}\times\sqrt{2})R45°$ geometry, according to our previous study.[12] The geometry of the upper layers corresponds to that of a slab of bulk acetylene, along the (010) direction.[17] Due to the very small mismatch between the KCl substrate and bulk acetylene this slab is assumed to be commensurate with the substrate, leading to one acetylene molecule per cation site in each layer of the slab. The total number of acetylene molecules varies then from 64 for 1 monolayer to 960 for 15 layers.

The molecular dynamics calculations are carried out by standard methods.[25] Each admolecule is treated as a rigid rotor and five external coordinates are used to describe the translation of the center of mass (x,y,z) and the orientation $[\mathbf{\Omega}=(\theta,\phi)]$ of the molecule. The substrate is also considered as a fixed body. The rotational equations of motion were solved by a leap-frog algorithm based on a quaternion representation of the molecular orientations, and a leap-frog extension to the method of Verlet was used for the translational equations of motion.[25] After 15 000 time steps of 2.2 fs each (corresponding to a real time of 33 ps) the system is equilibrated. The data were then collected for the next 15 000 steps. The initial linear and angular velocities were taken from a Boltzmann distribution corresponding to the desired simulation temperatures between 40 and 140 K. The temperature was held constant during the production run by scaling the velocities every 20 steps. Note that the equilibration of the system before collecting data prevents any significant temperature drift during the production phase. The scaling procedure used here is very smooth (less than 2 K) and we have checked that this procedure does not introduce artifacts due to the periodicity of the rescaling (every 20 steps).

For the interactions V^{MM} within the monolayer, which are calculated in the real space, a radial cutoff of 14 Å is used, whereas the binding potential V^{MS} is calculated in the reciprocal space of the substrate. Calculations of the lateral interactions within the adlayer were speeded up by using a neighbor list.[25] Preliminary tests were also performed at 40 K by using the Ewald scheme for the calculation of the lateral interactions. These tests showed that the Ewald method, which is much more time consuming, gives almost the same results as the summation in the real space.

C. Structural analysis and lattice dynamics of the adsorbate

The translational ordering of the acetylene molecules is studied as a function of temperature through the analysis of the distribution function $p(z)$, where z defines the distance between the KCl surface plane and the acetylene center of mass. In order to characterize the in-plane structure of the acetylene layers, a translational order parameter S_T is calculated using the following formula:

$$S_T(\mathbf{k})=\frac{1}{N}\left\langle\left|\sum_j e^{i\mathbf{k}\cdot\mathbf{r}_j}\right|\right\rangle, \tag{3}$$

where the summation accounts for the N molecules in the simulation box. The symbol $\langle\cdots\rangle$ means that an average is performed over the duration of the simulation. $\mathbf{r}_j$ defines the position of the center of mass of molecule j in the absolute

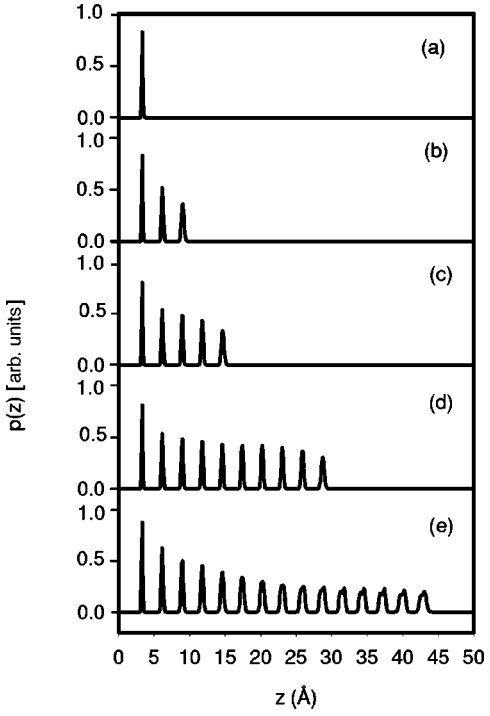

FIG. 7. Distribution function (in arbitrary units, a.u.) of the distance z(Å) of the acetylene molecular centers of mass from the KCl surface plane at $T=50$ K for (a) 64, (b) 192, (c) 320, (d) 640, and (e) 960 molecules in the simulation box.

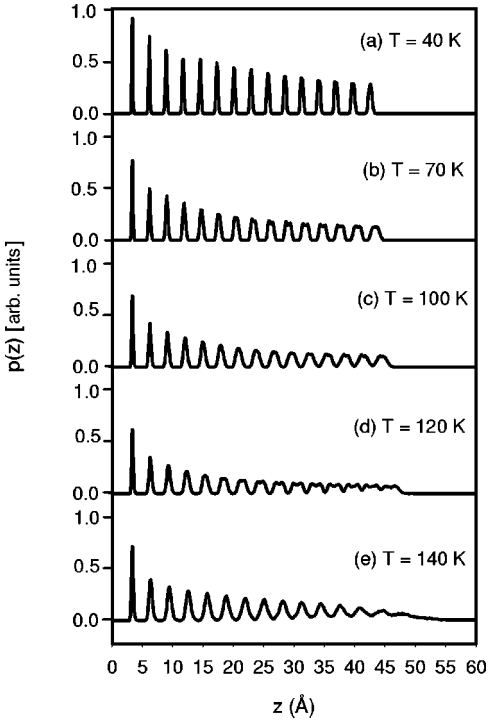

FIG. 8. Distribution function (in arbitrary units, a.u.) of the distance z(Å) of the acetylene molecular centers of mass from the KCl surface plane as a function of temperature for a coverage of 960 molecules in the simulation box (corresponding to 15 adlayers).

frame, and $\mathbf{k}=(2\pi/a,0,0)$ or $\mathbf{k}=(0,2\pi/a,0)$ are reciprocal lattice vectors parallel to the surface.

Similarly, the orientations of the acetylene admolecules are characterized at each temperature by the angular distribution functions $p(\theta)$ and $p(\phi)$, and the orientational disorder is monitored through the average cosine of the angle between the molecular axis and its equilibrium position in a bulk slab, as

$$S_R=\frac{\langle \mathbf{e}_j\cdot\mathbf{e}_j^0\rangle}{\langle \mathbf{e}_j^0\cdot\mathbf{e}_j^0\rangle}, \tag{4}$$

where $\mathbf{e}_j$ defines in the absolute frame a unit vector along the molecular axis of the jth acetylene admolecule and $\mathbf{e}_j^0$ is the corresponding vector in the perfectly ordered equilibrium initial configuration. The order parameters S_R and S_T characterize the displacements of the molecules from their ideal lattice positions. For the perfectly ordered structure at 0 K, they are equal to 1, whereas they tend to 0 for a completely disordered structure at high temperatures.

The phonon dispersion curves for an acetylene monolayer adsorbed on KCl have previously been calculated using quasiharmonic lattice dynamics.[12] For the adsorbed film the diagonalization of the dynamical matrix would not be tractable due to the large number of adsorbed layers. Instead, the dynamical information was extracted from the Fourier transform of autocorrelation functions, such as the velocity autocorrelation function (VACF) $[\langle \mathbf{v}(0)\cdot\mathbf{v}(t)\rangle]$ or the angular velocity autocorrelation function (AVACF) $[\langle \omega(0)\omega(t)\rangle]$ which, in the harmonic approximation, gives the one-phonon density of states for translational and orientational modes.[26,27] At the Brillouin zone center, this method usually leads to nice sharp peaks corresponding to the translational and orientational frequencies. A limitation of this method is that along the Brillouin zone, the frequency domain can be spread out and, as a consequence, it is rather difficult to assign modes.[28]

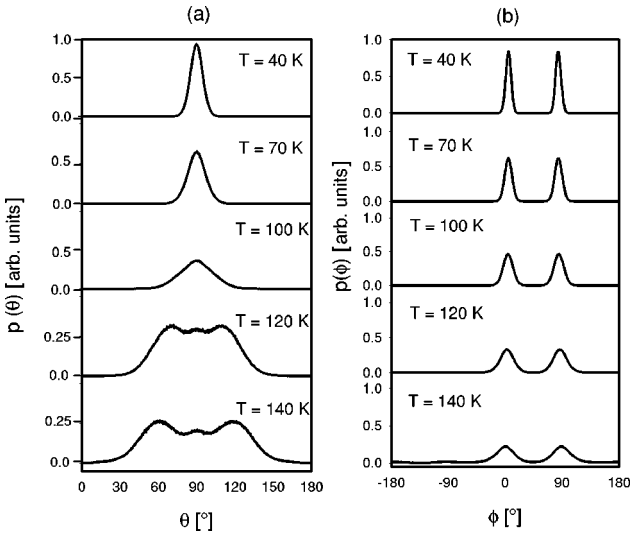

FIG. 9. Angular distribution functions (a) $p(\theta)$ and (b) $p(\phi)$ in arbitrary units (a.u.) for the acetylene molecules as a function of temperature, and for a coverage corresponding to 15 adlayers.

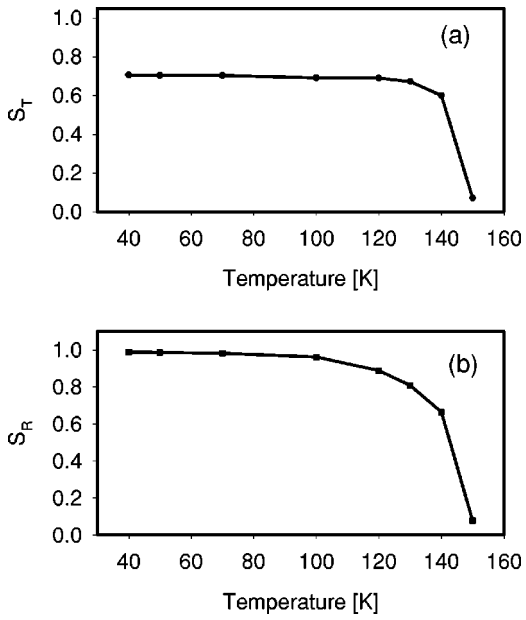

FIG. 10. (a) Translational and (b) orientational order parameters as a function of temperature, for a coverage corresponding to 15 adlayers.

IV. THEORETICAL RESULTS

A. Structure of the acetylene film

Molecular dynamics simulations were first performed for different acetylene coverages, at constant temperature. Figure 7 shows the distribution function $p(z)$ of the distance between the molecular centers of mass and the surface, at $T=50$ K with increasing acetylene coverage from $N=64$ to 960 molecules. For $N=64$ molecules, Fig. 7(a) exhibits a single sharp peak at $z=3.38$ Å which corresponds to the formation of the flat monolayer. The concomitant analysis of the angular distribution functions $p(\theta)$ and $p(\phi)$ indicates that this monolayer is characterized by a $(\sqrt{2}\times\sqrt{2})R45°$ geometry, as already obtained in our previous study.[12] When the coverage increases [Fig. 7(b) to Fig. 7(e)], the adsorbate exhibits a layer-by-layer arrangement, as shown by the occurrence of several single peaks with the same integrated intensity. The average layer spacing is 2.84 ± 0.06 Å. Each layer contains 64 molecules, which are oriented parallel to the KCl substrate as indicated by the occurrence of a single peak around 90° in $p(\theta)$ (not shown). This peak broadens with coverage, indicating that the parallel ordering is less and less pronounced as the z distance to the KCl surface increases. Moreover, the two peaks observed for all coverages in $p(\phi)$ (not shown) are characteristic of a $(\sqrt{2}\times\sqrt{2})R45°$ structure for each layer. For large distances between the admolecules and the substrate, i.e., $z>25.0$ Å, the tips of the peaks in $p(z)$ are split by about 0.6 Å [Fig. 7(e)]. This indicates that, at these distances, the admolecules in a given layer, do not lie in exactly the same plane. At $T=50$ K, the total (potential + kinetic) energy ranges between -24.0 kJ/mol for the monolayer and -16.2 kJ/mol for the thick film of 15 layers. The lateral interaction accounts for 38.5% of the total potential energy (-25.0 kJ/mol) within the monolayer, whereas for the thick film this contribution reaches 93.5% of the total energy

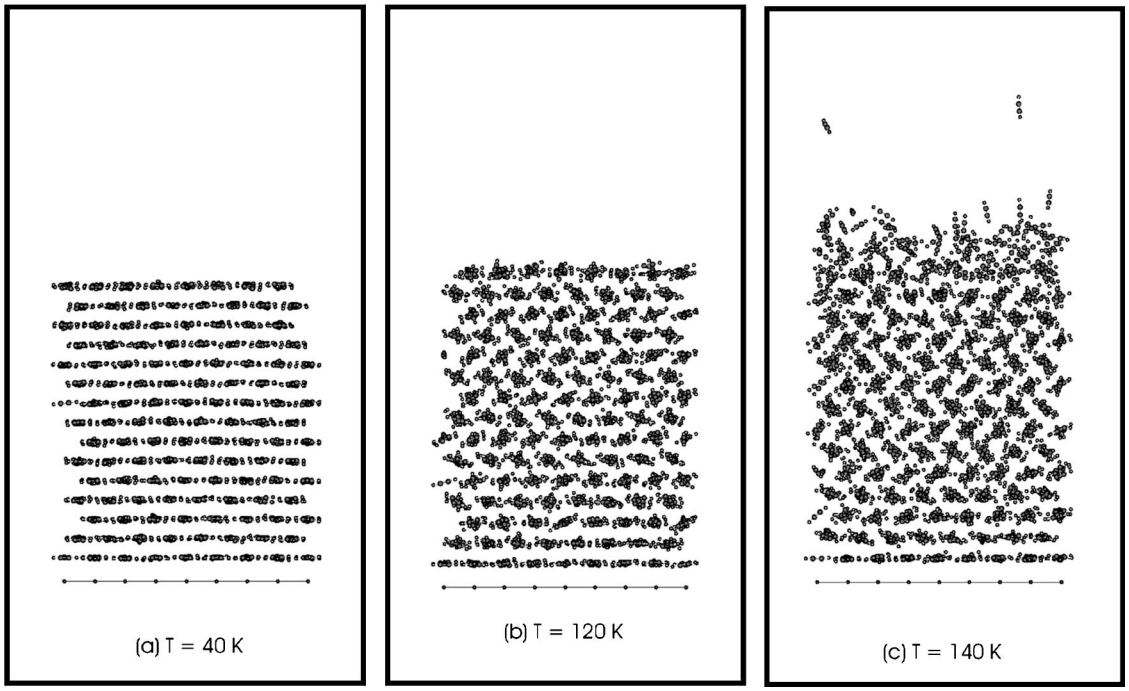

FIG. 11. Snapshots of the simulation with a coverage equal to 15 adlayers: side views at (a) 40, (b) 120, and (c) 140 K. The acetylene molecules form a commensurate thick film adsorbed above the KCl substrate. Note the parallel ordering of the different layers at $T=40$ K, and the effect of the phase transition on the orientational ordering of the upper layers at $T=120$ K. At $T=140$ K, desorption of acetylene molecules is observed. Only the KCl surface atoms are represented.

TABLE II. Calculated phonon-libron frequencies (meV) at the center of the Brillouin zone, for a monolayer at 50 K and for a thick film of 15 layers of acetylene at 40 K.

translation	ω (monolayer)	ω (film)	ω (surface layer)
x,y	3.5	2.0	2.0
	4.4		
	5.7	5.9	5.5
	8.6	7.7	6.8
	10.0	10.0	8.4
	11.1	11.8	10.5
	23.5		
z			2.0
		3.0	3.0
			4.7
		5.2	5.2
		7.7	
	10.4	10.0	
		11.8	
orientation			
Ω			4.7
		7.7	7.4
	10.4	10.0	
		11.8	12.1
		16.6	16.6
	18.0	19.1	19.1
	20.7		
	23.5	22.1	22.1
		26.0	25.0
e_z	3.5	3.0	3.0
	4.4	4.7	4.7
	5.7	6.8	6.8
		7.7	7.4
	10.0		10.5
	11.1	11.8	12.1
		13.6	
		15.1	
	23.5	26.0	

(-17.2 kJ/mol), indicating the vanishing influence of the interactions with the KCl substrate as the coverage increases.

In a second step, the MD simulations at constant coverage (namely 960 molecules) were used to study the structure and dynamics of a thick acetylene film when the temperature increases from $T=40$ K up to the desorption of the admolecules. The corresponding distribution function $p(z)$ is given in Fig. 8. At $T=40$ K, the adsorbed film corresponds to 15 parallel layers, separated by about 2.84 Å. Within these layers, the admolecules are adsorbed parallel to the KCl surface, as indicated by the occurrence of a single peak around 90° in $p(\theta)$ [Fig. 9(a)], and they are oriented perpendicular to each other [Fig. 9(b)] in order to form a $(\sqrt{2}\times\sqrt{2})R45°$ structure, as already observed at $T=50$ K. This ordering is maintained up to 100 K since no significant modification is found in the corresponding translational and orientational distribution functions (Figs. 8 and 9), except for a broadening of the different peaks, characteristic of large amplitude motions for the molecules pertaining to the outermost layers.

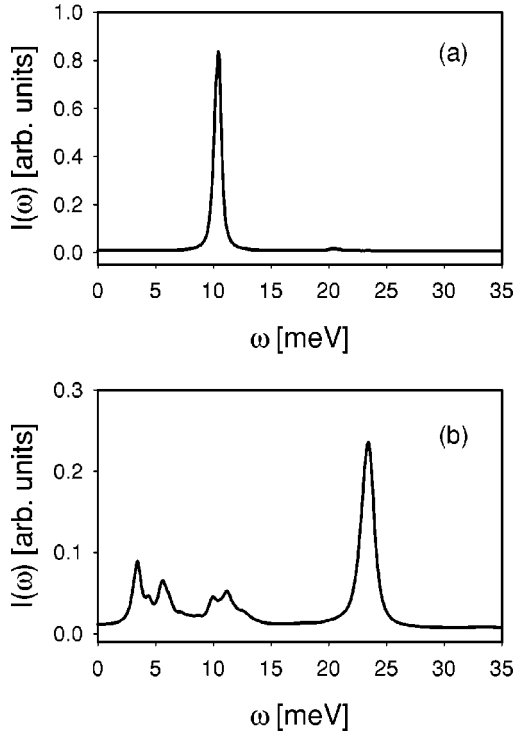

FIG. 12. Fourier transform (TF) of some autocorrelation functions for the C_2H_2 monolayer at 50 K (a) TF of $\langle v_z(0)v_z(t)\rangle$, (b) TF of $\langle e_z(t)e_z(0)\rangle$.

Above 100 K a phase transition occurs in the upper layers as indicated by the appearance of pronounced doublets in $p(z)$ for $z>15$ Å [Fig. 8(d)]. These doublets correspond to a bilayer arrangement of the admolecules, with a layer separation of about 1.3 Å. This phase transition is a consequence of the reorientation of the admolecules in the upper layers, which are no longer parallel to the KCl substrate, as shown by the two peaks appearing in $p(\theta)$ around 60° and 120° above 100 K [Fig. 9(a)]. The remaining third peak at $\theta=90°$ corresponds to acetylene molecules in the innermost layers which cannot reorient due to their proximity to the substrate. No change is observed in $p(\phi)$ at these temperatures [Fig. 9(b)], indicating that the relative orientation of the molecular axes is preserved in the whole film ($\Delta\phi=90°$).

Then, at $T=140$ K, the upper layers begin to melt as indicated by the coalescence of the bilayer peaks above $z\sim20$ Å [Fig. 8(e)]. Moreover, at this temperature, the long tail of $p(z)$ for $z>45$ Å indicates the onset of partial desorption of molecules of the outermost layer. Above 150 K the film is completely desorbed (not shown).

The translational S_T and orientational S_R order parameters for the thick film (15 layers) are displayed in Fig. 10 as functions of temperature. S_T and S_R remain nearly constant up to 100 K, indicating that parallel translational and orientational orders are maintained within the film in this temperature range. The orientational order present at low temperatures disappears above 100 K [Fig. 10(b)], whereas some parallel translational order remains up to 130 K [Fig. 10(a)].

This feature confirms that the phase transition occurring between 100 and 130 K is mainly of orientational nature, and does not affect the parallel ordering of the molecular centers of mass. Above 140 K, S_T and S_R abruptly decrease due to melting of the different layers and to concomitant partial desorption of the molecules.

From an energetic point of view, increasing the temperature does not appreciably affect the molecule-substrate interaction since it is limited to the innermost layers. It has a larger relative effect on the molecule-molecule contribution, which increases from -16.3 kJ/mol at $T=40$ K to -13.2 kJ/mol at $T=130$ K due to the structural changes within the upper layers. As a consequence, the total energy within the thick film increases from -16.6 to -11.6 kJ/mol within the temperature range (40–130 K), taking into account the additional effects of the temperature on the kinetic contribution. Note that above 130 K the snapshots taken from the simulations, shown in Fig. 11, indicate the desorption of the molecules and it is no longer possible to accurately calculate the total energy.

B. Lattice dynamics

The phonon-libron frequencies at the Brillouin zone center ($\bar{\Gamma}$ point) for the acetylene film adsorbed on KCl(001) were determined from the Fourier transform of the VACF's and AVACF's autocorrelation functions. The corresponding energies are listed in Table II for both the acetylene monolayer at $T=50$ K and the acetylene film (15 layers) at $T=40$ K. Due to the symmetry of the system at these temperatures, the translational frequencies calculated along the x and y directions are degenerate. Unfortunately with the technique used it was not possible to calculate the dependence of this mode frequencies on the wave vector. As said above, the mode energies correspond to the $\bar{\Gamma}$ point.

For the monolayer, the phonon-libron energies range between 3.5 and 23.5 meV. The translational motion perpendicular to the substrate is characterized by an energy of 10.4 meV, as deduced from the single peak in the Fourier transform of the z component of the velocity autocorrelation function [Fig. 12(a)]. The analysis of the other motions is more difficult [see, for example, Fig. 12(b)], since examination of Table II shows that the same energies are obtained from different autocorrelation functions. This indicates that hybridizations of the molecular motions occur due to the dynamical couplings in the adsorbate. For example, translational (x,y) motions parallel to the surface and perpendicular orientation of the molecular axes (e_z) are characterized by the same energy values, at 3.5, 4.4, 5.7, 10.0, 11.1, and 23.5 meV [Fig. 12(b)]. This coupling indicates that parallel translation of the center of mass is accompanied by a reorientation of the molecular axis in the plane perpendicular to the surface, as an effect of the strong trapping above the surface cations. Furthermore, the mode obtained at 8.6 meV and the two modes calculated at 18.0 and 20.7 meV are related to pure parallel translational and pure orientational motions, respectively, since they do not appear in the other autocorrelation functions. Note that the frequencies which appear in the analysis of both translational and orientational motions (23.5 meV, for example) are independent of the temperature rescaling procedure. This indicates that these frequencies are truly characteristic of coupled motions and do not come from artificial periodicity.

For the 15 layers film the translational and orientational energies were calculated separately for the entire film and for the molecules in the outermost layer (see Table II). The comparison between the second (entire film) and the third (surface layer) columns of Table II indicates that the dynamics of the outermost layer is different from that of the innermost layers, as indicated by the presence of different modes in the simulations. For example, three translational modes are obtained for the whole film at 7.7, 10.0, and 11.8 meV, which are not present for the surface layer, and thus they must correspond to bulk modes. This conclusion is reinforced by the fact that these modes are obtained from the Fourier transform of each component (v_x,v_y, and v_z) of the VACF's, indicating that they correspond to isotropic motions within bulk layers. Since these modes are also obtained in the analysis of the orientational motions, they indicate a translation-orientation coupling. For bulk layers, three additional pure orientational modes are also calculated at 13.6, 15.1, and 26.0 meV, corresponding to two perpendicular and one parallel mode, respectively.

The other translational and orientational modes are rather characteristic of the surface layer motions since they are obtained in dynamical analysis of both the whole film and the outermost layer. Modes at 5.5 and 8.4 meV correspond to a purely parallel translation, whereas the mode at 5.2 meV is due to purely perpendicular translation of the molecules pertaining to the outermost layer. The coupling between the parallel and perpendicular translational motions gives rise to the additional mode at 2.0 meV. In the same way, pure orientational modes for the surface layer are obtained at 7.4, 12.1, 16.6, 19.1, 22.1, and 25.0 meV, with the three highest energy modes characterizing parallel motions, whereas those at 7.4 and 12.1 meV correspond to a coupling between the parallel and perpendicular orientations. Modes at 3.0 and 4.7 meV are due to coupling between perpendicular translational and orientational motions, whereas the remaining modes at 6.8 and 10.5 meV correspond to coupling between parallel translations and perpendicular orientational motions within the outermost layer.

Finally, it should be noted that the coupled translational/orientational motions within the bulk adlayers are characterized by slightly higher energies (7.7, 10.0, and 11.8 meV) than the corresponding motions within the outermost layer (6.8, 8.4, and 10.5 meV), as a consequence of the reduced coordination of the admolecules.

V. DISCUSSION AND COMPARISON WITH THE EXPERIMENTS

Previous simulations[12] have shown that acetylene molecules can form a perfectly ordered monolayer on the KCl substrate, characterized by a $(\sqrt{2}\times\sqrt{2})R45°$ geometry containing two molecules per unit cell, related by a glide plane. The present calculations, which are based on a different description of the lateral interactions between C_2H_2 molecules

in order to have a better description of the acetylene dynamics,[23,24] confirm the stability of this monolayer geometry. The main difference between the two studies concerns the smaller contribution of the lateral interactions, which represents about 38% of the total potential energy in the present calculations, instead of about 50% in the previous study. As a consequence, the total adsorption energy is equal to -24 kJ/mol at $T=50$ K, instead of -29 kJ/mol at $T=40$ K in the previous study. These results are in fair agreement with the HAS data regarding both the geometry of the acetylene monolayer and the value of the heat of adsorption (-27 ± 1 kJ/mol).

In the present paper, the structure and dynamics of the acetylene adsorbate have been investigated at higher coverages. Simulations with increasing number of acetylene molecules in the MD box at $T=50$ K show that the admolecules are regularly organized within several parallel layers (up to 15 layers for the thicker film considered here), maintaining the $(\sqrt{2}\times\sqrt{2})R45°$ geometry up to the outermost layer. Such a feature is fully consistent with the experimental observation of a layer-by-layer growth for the acetylene molecules when the coverage is increased, as well as with the HAS data showing no significant changes in the diffraction pattern with respect to the monolayer.

For a thick film (15 layers), the $(\sqrt{2}\times\sqrt{2})R45°$ translational structure remains stable up to about 130 K, while an orientational transition occurs around 100 K in the outermost layers, which is characterized by a tilt of the molecular axis out of the (x,y) surface plane (θ angle). This transition appears to be similar to the transition from the orthorhombic to the cubic phase observed for bulk acetylene around 133 K.[17] The ''incomplete'' transition observed in the present simulations is due to the substrate influence which strongly maintains the innermost layers of the film parallel to the solid surface of KCl. Finally, melting of the layers, followed by desorption of the acetylene molecules are also observed above 140 K. However, under the experimental conditions desorption is observed at $T_S=81-82$ K and therefore the transition cannot be studied directly.

At $T=40$ K, the calculated total energy of the acetylene film is about -17.0 kJ/mol. Since the contribution of the molecule-substrate interaction is expected to be relatively small, it is not surprising that this result compares very well with the bulk acetylene energy calculated with the same lateral interaction potential [-18 kJ/mol (Ref. 23)]. Unfortunately the total energy is much smaller than the measured desorption energy of 24 kJ/mol. This discrepancy indicates that improvements are certainly needed in the description of the lateral interactions.

The calculated phonon-libron energies at the $\overline{\Gamma}$ point cannot be compared directly with the experimental data since on one hand the dispersion curves along the entire Brillouin zone have not been determined in the calculations, and on the other hand, the experimental resolution was not always sufficient to resolve close lying modes. Moreover, sometimes modes are not seen at the zone center.

The modes calculated at 3.5, 4.4, and 5.7 meV result from coupling between parallel translation and perpendicular orientational motions and should be compared with the measured data at about 3.0 and the two modes at about 7.0 meV (E_1, E_2, E_3), which also exhibit perpendicular polarization. Four additional modes are also calculated between 8.6 and 11.1 meV, corresponding either to pure parallel translational motion (8.6 meV), or to pure perpendicular translational motion (10.4 meV), or to a coupling between parallel translations and perpendicular orientation (10.0 and 11.1 meV). In the experiments, only one mode (E_4) is observed in this energy range, but the scatter of the data for small parallel momentum transfers may suggest that more than one single mode is measured near the BZ center, between 8.0 and 10.5 meV. For example, the purely perpendicular translational mode calculated at 10.4 meV and the coupled mode at 10.0 meV should have been observed in the experiments, since the helium probe is strongly sensitive to perpendicular motions. The low incident energy of the helium beam prevents the observation of the higher energy modes at 18.0, 20.7, and 23.5 meV.

The present calculations are consistent with our previous study of the dynamics of the C_2H_2 monolayer on KCl(001), based on the dynamical matrix formalism,[12] and using a different potential for the description of the lateral interactions. In the previous work it was shown that modes E_1 and E_2 correspond to hybridization between parallel and perpendicular motions at the $\overline{\Gamma}$ point, as obtained here. The E_3 mode at 8.8 meV which previously was attributed to purely parallel translations could also be related to the parallel translational mode calculated in the present study at 8.6 meV. But, in this case, a strong coupling with the substrate modes must be invoked in order to explain the clear appearance of this mode in the experiments. One may then wonder whether the 8.6 meV mode might instead be related to the perpendicular modes calculated at 10.0 and 10.4 meV. Since the calculations are for a rigid substrate, the perpendicular polarized modes will be overemphasized. Finally, the use of a different model for the description of the lateral interactions (distributed multipole model in the present simulations, point quadrupole at the center of mass in the previous study) could explain the slight differences in the calculated energies between the two studies, especially regarding the parallel orientational modes.

For the thick film, the energies of the different modes calculated in the present simulations at $T=40$ K can help in the interpretation of the experiments. For example, the nondispersive mode observed around 3.0 meV in the experiments can be assigned to the mode calculated at the same energy, which corresponds to a coupling between perpendicular translational and perpendicular orientational motions of the admolecules within the outermost layer of the film. In the same way, the other perpendicularly polarized modes at 4.7 meV (translation + orientation) and 5.2 meV (pure translation) appear to correspond to the scattered points observed around 5.0 meV in the data. In the calculations, additional modes are obtained at 6.8, 7.4, and 7.7 meV, corresponding to coupling between translational and orientational motions. These modes, which are characterized by a perpendicular polarization, should be visible in the experiments, and thus, could be related to the mode measured between 6.5 and 7.0

meV in the experiments. Finally, the experimentally observed mode at about 9.0 meV could be attributed to the calculated mode at 10.0 meV, which exhibits also a perpendicular polarization, and corresponds to a coupled translational and orientational motion. Note that it is not expected that the other calculated modes with pure parallel polarization, or with higher energy can be observed in the experiments.

Despite the neglect of the substrate lattice dynamics in the calculations, which should have a great influence at low coverage, the good agreement between simulations and experiments indicates that the potential used in the present calculations is rather suitable for describing the dynamics of the admolecules. However, it appears less accurate from an energetic point of view. This is not surprising since the model used in this paper for describing the lateral interactions has been optimized for the calculations of the bulk acetylene dynamics,[23] rather than for the calculation of the total energy.

VI. CONCLUSIONS

Multilayers of acetylene on KCl(001) have been investigated by He-atom scattering and molecular dynamics calculations. During isothermal adsorption of acetylene on KCl(001) at $T_S = 40$ K layer-by-layer growth up to at least 15 layers C_2H_2 is observed. From He diffraction a $(\sqrt{2} \times \sqrt{2})R45°$ symmetry of the surface unit cell with glide planes along the $\langle 100 \rangle$ directions has been determined for the 15 layer films. This is consistent with a face of the orthorhombic modification of bulk acetylene. The surface phonon dispersion curves show the Rayleigh mode of the acetylene surface as well as at least three further modes below 10 meV.

The calculations agree with the experiments very well regarding the structure of the layers and their tendency to exhibit layer-by-layer growth. The dynamical properties have been calculated from the Fourier transform of autocorrelations functions and provide a plausible assignment of the experimental E_1-E_4 modes to different coupled translational and orientational motions of the surface molecules.

ACKNOWLEDGMENTS

The authors would like to thank Professor L. W. Bruch for discussions about the theoretical approach as well as Dr. E. Hulpke for many helpful discussions of experimental problems.

*Corresponding author.

[1] L. W. Bruch, Milton W. Cole, and Eugene Zaremba, *Physical Adsorption: Forces and Phenomena* (Clarendon Press, Oxford, 1997).
[2] S. Keith Dunn and G.E. Ewing, J. Vac. Sci. Technol. A **11**, 2078 (1993).
[3] S.K. Dunn and G.E. Ewing, J. Phys. Chem. **96**, 5284 (1992).
[4] B.N.J. Persson, E. Tosatti, D. Fuhrmann, G. Witte, and C. Wöll, Phys. Rev. B **59**, 11 777 (1999).
[5] M. Lee, J.H. Schön, Ch. Kloc, and B. Batlogg, Phys. Rev. Lett. **86**, 862 (2001).
[6] J.H. Schön, C. Kloc, and B. Batlogg, Nature (London) **406**, 702 (2000).
[7] M. Bienfait, Europhys. Lett. **4**, 79 (1987).
[8] J.P. Coulomb, M. Maclih, B. Croset, and H.J. Lauter, Phys. Rev. Lett. **54**, 1536 (1985).
[9] J.M. Gay, J. Suzanne, and J.P. Coulomb, Phys. Rev. B **41**, 11 346 (1990).
[10] A. Glebov, R.E. Miller, and J.P. Toennies, J. Chem. Phys. **106**, 6499 (1997).
[11] S. Picaud, P.N.M. Hoang, C. Girardet, A. Glebov, R.E. Miller, and J.P. Toennies, Phys. Rev. B **57**, 10 090 (1998).
[12] A. Glebov, V. Panella, J.P. Toennies, F. Traeger, H. Weiss, S. Picaud, P.N.M. Hoang, and C. Girardet, Phys. Rev. B **61**, 14 028 (2000).
[13] J. P. Toennies, in *Surface Phonons, Springer Series in Surface Science* No. 21, edited by W. Kress and F. W. deWette (Springer, Berlin, 1991).
[14] J.P. Toennies and R. Vollmer, Phys. Rev. B **44**, 9833 (1991).
[15] B. Poelsema and G. Comsa, *Scattering of Thermal Energy Atoms from Disordered Surfaces, Springer Tracts in Modern Physics* No. 115 (Springer, Berlin, 1989).
[16] P.A. Redhead, Vacuum **12**, 203 (1962).
[17] R.K. McMullan, A. Kvick, and P. Popelier, Acta Crystallogr., Sect. B: Struct. Sci. **48**, 726 (1992).
[18] F. Traeger, Ph.D. thesis, Göttingen, 2001.
[19] E. Hulpke, J. Lower, and A. Reichmuth, Phys. Rev. B **53**, 13 901 (1996).
[20] Z. Gamba and H. Bonadeo, J. Chem. Phys. **76**, 6215 (1982).
[21] G. Lange, D. Schmicker, J.P. Toennies, R. Vollmer, and H. Weiss, J. Chem. Phys. **103**, 2308 (1995).
[22] D. Ferry and J. Suzanne, Surf. Sci. **345**, L19 (1996).
[23] J.W. Leech and P.J. Grout, J. Phys.: Condens. Matter **5**, 1299 (1993).
[24] F.L. Hirshfeld and K. Mirsky, Acta Crystallogr., Sect. A: Cryst. Phys., Diffr., Theor. Gen. Crystallogr. **35**, 366 (1979).
[25] M. P. Allen and D. J. Tildesley, *Computer Simulations of Liquids* (Clarendon, Oxford, 1987).
[26] R. M. Lynden-Bell (private communication).
[27] R.M. Lynden-Bell, R.W. Impey and M.L. Klein, Chem. Phys. **109**, 25 (1986).
[28] L. W. Bruch (private communication).